



## Section 2. Chemistry biology

DOI:10.29013/EJBLS-24-3-21-38



### IDENTIFYING CEACAM 1-TARGETED DRUG CANDIDATES FOR CANCER IMMUNOTHERAPY

*Guanrong (Rain) Cheng*<sup>1</sup>

<sup>1</sup> Garden International School, Malaysia

---

**Cite:** *Guanrong (Rain) Cheng. (2024). Identifying Ceacam1-Targeted Drug Candidates For Cancer Immunotherapy. The European Journal of Biomedical and Life Sciences 2024, No 3. <https://doi.org/10.29013/EJBLS-24-3-21-38>*

---

#### Abstract

Carcinoembryonic antigen-related cell adhesion molecule 1 (CEACAM1) is a key regulatory protein in immune modulation and tumor progression, making it a promising target for cancer immunotherapy. Immunotherapy is promising because it harnesses the body's own immune system to identify and eliminate cancer cells, often leading to more durable responses compared to traditional therapies like chemotherapy and radiation. By targeting immune checkpoints, such as those regulated by CEACAM1, immunotherapy can reinvigorate exhausted immune cells, enhancing their ability to fight tumors. CEACAM1 is particularly promising as a target because it plays a key role in immune checkpoint pathways that tumors exploit to evade immune detection. By interacting with immune cells, CEACAM1 can inhibit the immune response against tumors, allowing them to grow unchecked. This study uses computational docking methods to evaluate potential interactions between CEACAM1 and a variety of compounds from the ZINC database. The docking process involved multiple steps, including target and ligand selection, docking simulation, and binding affinity calculation. SwissADME and ProTox 3.0 tools were employed to assess the drug-like properties and toxicity profiles of the top candidates. From an initial pool of 20 compounds, five candidates had the most favorable binding energies ( $\Delta G$ ). Further analysis revealed that while ZINC71788521 and ZINC67902861 exhibited good target affinity, they violated Lipinski's rule of five. Conversely, ZINC08820313, ZINC38617077, and ZINC41591046 adhered to Lipinski's rule, demonstrating promising drug-like characteristics. In the end, ZINC08820313 was chosen as a potential drug candidate due to its high  $\Delta G$  and low toxicity levels compared to the other compounds chosen. The study identifies potential CEACAM1 inhibitors with favorable energetic interactions and acceptable drug-like properties. Future work will involve in vitro and in vivo validation to substantiate these computational predictions.

**Keywords:** *Cancer, CEACAM1, Immunotherapy, Immune checkpoints, Drug candidates*

### Introduction:

Cancer is a broad group of diseases characterized by uncontrolled cell growth and the ability of those cells to invade other tissues. There are over 200 different types of cancer affecting various parts of the body (Cancer Research UK, 2023). Common cancer treatment approaches include surgery, radiation, chemotherapy, targeted therapy, immunotherapy and combinations of these which are normally referred to as combination therapy. These therapies each have distinct mechanisms and limitations, such as surgery and radiation, which are often localized treatments, while chemotherapy uses drugs to target rapidly dividing cells, affecting both cancerous and healthy cells. Modern treatments allow many people to survive cancer, seen through the increase of 5-year survival rate for lung and bronchus cancer from 20.5% in 2010–2016 (Chaitanya Thandra et al., 2021) to 26.7% in 2024 (National Cancer Institute, 2018). However, cancer still remains one of the leading causes of death worldwide. The development of new and more effective therapies is an active area of research, with combination treatments of targeted therapy and immunotherapy showing particular promise due to them being specific to the cell or protein.

Immunotherapy is a form of treatment that uses the body's own immune system to fight disease. It presents new opportunities for more effective and less toxic cancer therapies by enhancing existing anti-tumor immune responses or counteracting strategies employed by tumors to evade immunity (Zhang & Zhang, 2020). Different types of cancer immunotherapies include monoclonal antibodies, immune checkpoint inhibitors, cancer vaccines, and adoptive cell therapies. Immune checkpoint inhibitors in particular are one of the more powerful approaches in immunotherapy, producing durable responses in around 20–25% of patients with advanced melanoma, non-small cell lung cancer, and other cancers (Hodi et al., 2010). However, response rates can vary significantly across different cancer types, with checkpoint inhibitors showing the most benefit in cancers with a high mutational burden like melanoma and lung cancer, and less efficacy in cancers like prostate cancer (Zappasodi et al., 2018).

Immune checkpoints are regulatory proteins expressed on immune cells that act as stimulatory or inhibitory switches to modulate the immune response (Alsaab et al., 2017). Well-known examples of inhibitory immune checkpoints include CTLA-4, PD-1, TIM-3, LAG-3, and VISTA. CTLA-4 is expressed on activated T cells and inhibits early stages of T cell activation. PD-1 is induced on activated T cells, B cells, and myeloid cells and inhibits effector functions in peripheral tissues (Pauken and Wherry, 2015). In normal physiology, immune checkpoints play an important role in preventing autoimmunity by raising the threshold for T cell activation and proliferation, thereby limiting chronic inflammation and autoimmune damage to healthy cells (Darvin et al., 2018). They provide inhibitory signals that counterbalance costimulatory signals, maintaining self-tolerance and modulating the intensity and duration of immune responses against foreign antigens (Buchbinder and Desai, 2016).

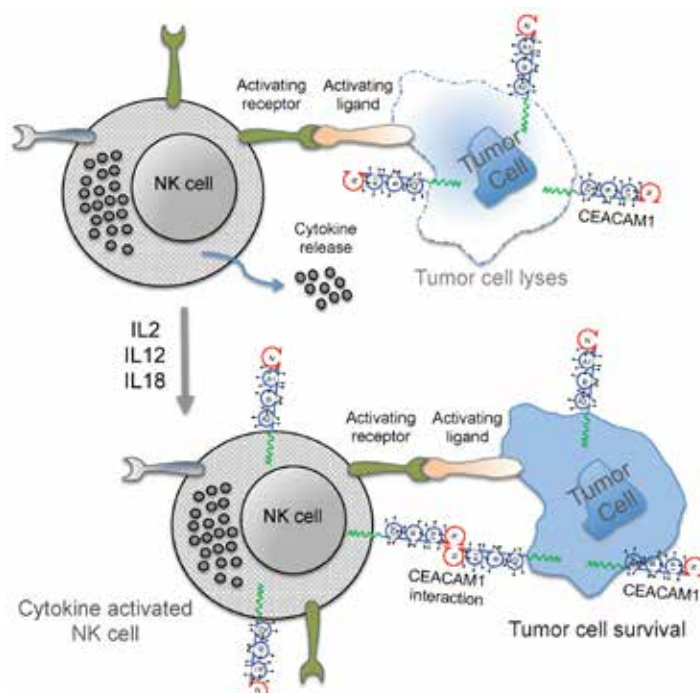
Carcinoembryonic antigen-related cell adhesion molecule 1 (CEACAM1) is a transmembrane glycoprotein of the immunoglobulin superfamily that plays roles lots of functions in the human body such as cell adhesion, angiogenesis, insulin metabolism, and immune regulation (Kim et al., 2019). It is widely expressed on epithelial cells, endothelial cells, and immune cells including T cells, B cells, and natural killer (NK) cells (Tucru et al., 2016). CEACAM1 functions by mediating homotypic and heterotypic cell-cell adhesion interactions through binding to other CEACAM family members or integrin receptors (Klaile et al., 2009). Its expression is highly regulated, with different isoforms generated by alternative splicing and its presence modulated by cytokines and other factors (Nagaiishi et al., 2008). Other than homophilic binding, CEACAM1 also binds heterophilically to CEACAM5, CEACAM6, and CEACAM8 (Kim et al., 2019), as well as integrin receptors like  $\alpha\beta3$  (Brümmer et al., 2001).

CEACAM1 has a strong relationship with both cancer progression and suppression. Upregulation of CEACAM1 is observed in many cancers like colon, breast, prostate, and non-small cell lung cancer, and increased CEACAM1 expression correlates with higher tumor stage, metastasis, and poor prognosis

(Danker et al., 2017). CEACAM1 promotes tumor angiogenesis by disrupting endothelial cell-cell junctions and enhancing vascular permeability (Horst et al., 2009). It also facilitates immune evasion by inhibiting tumor-killing by NK cells and cytotoxic T cells (Markel et al., 2009). However, CEACAM1 can also have tumor suppressive effects by inducing anoikis and impairing anchor-

age-independent growth (Benchimol et al., 1989). This dual role makes CEACAM1 an attractive cancer target, as inhibition could simultaneously block tumor angiogenesis and immune evasion while enhancing anoikis. Indeed, anti-CEACAM1 monoclonal antibodies enhance anti-tumor immunity and inhibit metastasis in preclinical models (Danker et al., 2017).

**Figure 1.** NK cells activated by CEACAM1 (top). CEACAM1 expressed by NK cells reduces the NK cells' ability to kill tumor cells (bottom). Figure obtained from (Helfrich et al., 2019)



### Literature review:

Park and coauthors observed in hepatocellular carcinoma (HCC), CEACAM1 is a promising target due to its role in regulating immune cell functions. CEACAM1 expression is significantly upregulated in EpCAM+ cancer stem cells, which are typically resistant to NK cell-mediated cytotoxicity. Targeting CEACAM1 in these cells has shown potential to enhance NK cell effectiveness, showing that blocking CEACAM1 in EpCAM-high HCC cells increases NK cell degranulation and cytotoxicity. Moreover, the knock-down of CEACAM1 using shRNA has been found to reduce its expression, therefore improving the susceptibility of tumor cells to immune-mediated killing (Park et al., 2020).

Tsang and coauthors have developed a monoclonal antibody named NEO-201, which

specifically binds to CEACAM-5, a glycoprotein often overexpressed in various carcinomas including colorectal, gastric, pancreatic, non-small cell lung, and breast cancers. The binding of NEO-201 to CEACAM-5 inhibits its interaction with CEACAM-1, another cell adhesion molecule found on NK cells. This inhibition is significant because the CEACAM-5/CEACAM-1 interaction typically suppresses the cytotoxic activity of NK cells against tumor cells. By blocking this interaction, NEO-201 can potentially restore and enhance the ability of NK cells to kill tumor cells. Moreover, NEO-201 exhibits direct anti-tumor activity through mechanisms such as antibody-dependent cell-mediated cytotoxicity (ADCC) and complement-dependent cytotoxicity (CDC). These processes involve the recruitment of immune cells and the activation of the complement

system to target and destroy tumor cells expressing CEACAM-5 (Tsang et al., 2022).

These findings suggest that CEACAM1-targeted therapies could potentially boost the body's anti-tumor immune response by modulating the interactions between CEACAM1 and immune cells, such as CD8+ T-cells and NK cells. By enhancing the cytotoxic activity of these immune cells and overcoming cancer stem cell-mediated resistance, CEACAM1-targeted approaches improve the efficacy of existing cancer treatments. However, the studies discussed previously are focused on specific cancer types (melanoma and HCC), and further research is needed to understand the broader applicability of CEACAM1-targeted therapies across different cancer types and in combination with other therapies.

### **Methodologies:**

#### ***Analysis of Binding Sites in CEACAM1:***

##### *Geometric method:*

1. Open chrome browser
2. Enter the link <https://proteins.plus/> in the browser and enter
3. Type in the PDB-Code 5DZL
4. Click "Go!"
5. Click "DoGSiteScorer Binding site detection"
6. Click "DoGSiteScorer"
7. Click "Calculate"
8. Click on the eye icon in the second column to visualize the binding sites

##### *Energetic-based method:*

1. Open chrome browser
2. Enter the link <https://ftsites.bu.edu/> in the browser and enter
3. Enter job name
4. Type in the PDB-Code 5DZL
5. Type in the email address
6. Click "Find My Binding Site"
7. Wait for the job complete email
8. Download the attachment in the email
9. Click on the link in the email
10. Click "Finish"

##### *Machine learning method:*

1. Open chrome browser
2. Enter the link <https://prankweb.cz/> in the browser and enter
3. Type in the PDB-Code 5DZL
4. Click "Submit"

#### ***Obtaining compounds that binds to CEACAM1***

##### *Virtual Screening*

1. Open chrome browser
2. Enter the link <http://pocketquery.csb.pitt.edu/> in the browser and enter
3. Click "Search"
4. Enter PDB ID7RQR4
5. Click "Search"
6. Choose cluster in B chain with a score closest to 1.0
7. Click "Export"
8. Click "Send to ZINCPharmer"
9. Go to the viewer tab
10. Unselect "Ligand" and "Receptor Residues"
11. If less than 3 pharmacophore visible, choose a different cluster
12. Click "Submit Query"
13. If no matches found, unselect one of the pharmacophore that is the furthest away from the rest in the pharmacophore tab and click "Submit Query" again
14. Choose the compounds with RMSD closest to 0.0
15. Repeat until 20 compounds chosen

#### ***Quantifying the energy between the interaction of compounds obtained and CEACAM1***

##### *Molecular Docking*

1. Open chrome browser
2. Enter the link <https://zinc12.docking.org/> in the browser and enter
3. Paste in one of the ZINC id from experiment 3.2.1. in the "Quick Search" bar and click "Go"
4. Copy the SMILES formate
5. Open another tab
6. Enter the link <https://datascience.unm.edu/tomcat/biocomp/convert> in the browser and enter
7. Under "Input" in the "Format" section, select "smiles – SMILES"
8. Under "Output" in the "Format" section, select "mol2 – Tripos mol2"
9. Under "Output" in the "generic" section, select "+3D"
10. Paste the SMILES format from step 4 in the box under "Input"
11. Click "Go Convert"
12. Click "download convert\_out.mol2"
13. Rename the file into the ZINC id
14. Open another tab



15. Enter the link <http://old.swissdock.ch/docking> in the browser and enter
16. Under “Target selection” click “upload file”
17. Click “Choose file”
18. Upload file with PDB code of 5DZL
19. Under “Ligand selection” click ‘upload file”
20. Click “Choose file”
21. Choose the file renamed in step 13
22. Make sure it says “Successful setup” under both “Target selection” and “ligand selection”
23. Enter job name
24. Enter email
25. Click “Start Docking”
26. Wait for Job Terminated email
27. Click on the link attached in the Job Terminated email
28. Find the highest estimated  $\Delta G$
29. Repeat for 20 compounds and select 5 with the highest estimated  $\Delta G$  compared to others for the next experiment

#### **Drug properties**

##### *SwissADME*

1. Collect and copy the SMILES code of the compound selected in 3.3.1.
2. Open Firefox browser
3. Enter the link <http://www.swissadme.ch/> and enter
4. Paste in the SMILES formate in the box
5. Press “Run!” and wait for results

#### **Toxicity prediction**

##### *ProTox 3.0*

1. Select the compound from experiment 3.4.1. that had no violations in Lipinski’s rule of 5
2. Open Firefox browser
3. Enter the link <https://tox.charite.de/protox3/index.php?site=home#> and enter
4. Click on the box with orange borders titled “Tox Prediction”
5. Paste in the SMILES format of compound selected in the “Canonical Smiles” section
6. Click on “smiles”
7. Scroll down to select models to predict, click “all”
8. Click “Start Tox-Prediction”

#### **Results and Discussion:**

#### ***Analysis of Binding Sites in CEACAM1:***

##### *Geometric method:*

Using the geometric method, ProteinPlus identified ten potential binding sites in CEACAM1. The most promising site, P\_0, displayed the largest volume (1177.38 Å<sup>3</sup>) and surface area (1364.93 Å<sup>2</sup>), coupled with the highest drug score (0.78) and simple score (0.62), which may suggest its suitability for drug binding. Other promising sites include P\_1 and P\_2, which also had relatively high volumes and scores, suggesting they could be viable targets as well. However, sites like P\_4 through P\_9 had significantly lower scores and smaller volumes, making them less favorable for drug binding. The results indicate there are many binding sites in CEACAM1, therefore making it a very promising drug target.

**Figure 2.** 10 possible binding sites in CEACAM 1(PDB code: 5DZL) detected by ProteinPlus based on size

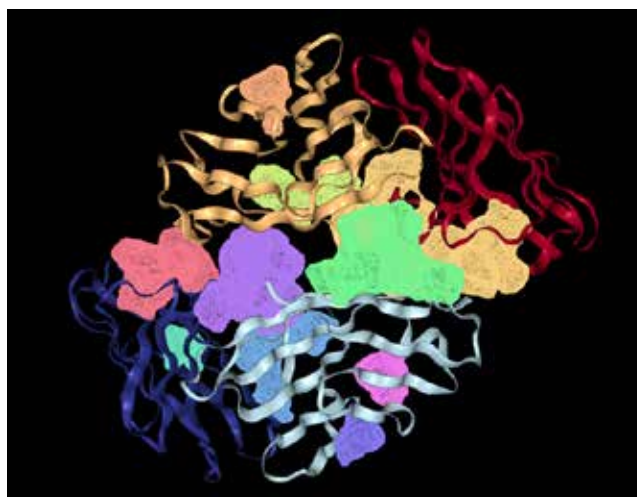


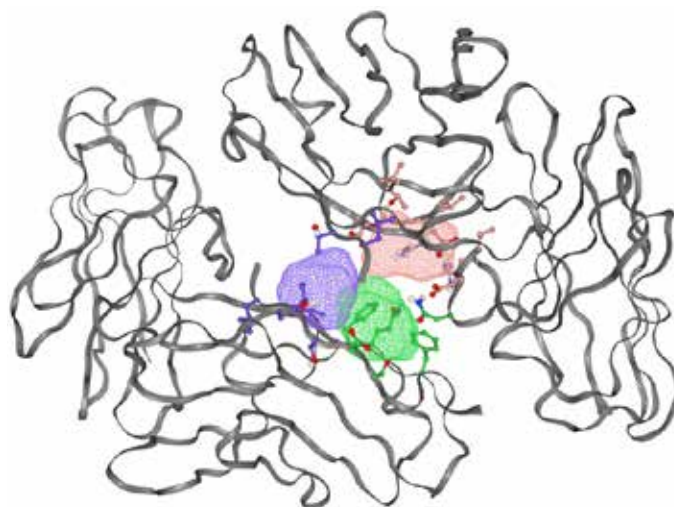
**Table 1.** Binding sites predicted by ProteinPlus in CEACAM1(PDB code: 5DZL).

Color	Name	Volume(Å <sup>3</sup> )	Surface Area(Å <sup>2</sup> )	Drug Score	Simple Score
Yellow	P_0	1177.38	1364.93	0.78	0.62
Purple	P_1	953.32	1102.57	0.76	0.59
Green	P_2	709.25	919.7	0.72	0.49
Red	P_3	477.3	609.26	0.64	0.27
Blue	P_4	349.02	549.5	0.46	0.12
Lime Green	P_5	202.01	496.25	0.42	0.01
Magenta	P_6	170.04	286.83	0.3	0.0
Cyan	P_7	117.07	152.53	0.38	0.0
Orange	P_8	110.63	273.66	0.27	0.0
Dark Blue	P_9	100.55	212.03	0.2	0.0

*Energetic-based method:*

Using an energetic-based method, FT Site detected 3 possible binding sites on CEACAM1. This method assesses binding affinity or energy between a molecule and a target site. FT Site can calculate and predict

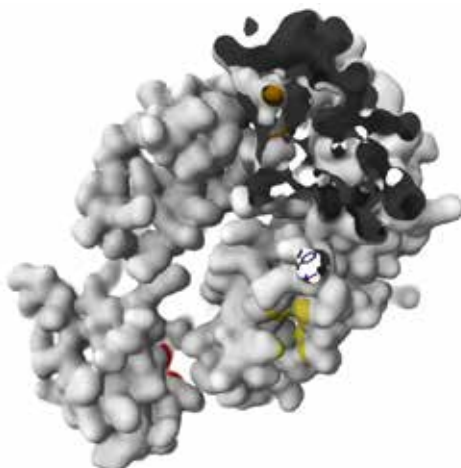
the interaction energy based on the physical and chemical properties of the molecules involved. The results suggest that 3 binding sites have enough energy to successfully allow molecules to bind to, which further confirmed CEACAM1 is a promising drug target.

**Figure 3.** 3 possible binding sites in CEACAM 1(PDB code: 5DZL) detected by FT Site based on energetic-based method*Machine learning method:*




Using a machine learning method, Prankweb detected 3 possible binding sites for CEACAM1. The most promising binding site, coloured red and ranked 1, has a score of 4.04 and 11 residues. This means through analyzed data and predictions made based on patterns and statistical models, the red binding site predicted binding affinity is the highest. Furthermore, 11 residues suggests that there is a large area for potential interactions. Yellow and orange binding sites are

ranked 2 and 3 respectively, with a score 2.27 and 1.09. These are both decent scores which conveys of them being a promising target. In this method, the promising targets found are more spread out around the sides of CEACAM1. However, in the energetic-based method, the promising targets are found close to the center of CEACAM1. This shows the large variety of binding sites in CEACAM1, which suggests that it will be a highly promising target.

**Figure 4.** 3 possible binding sites in CEACAM 1 (PDB code: 5DZL) detected by Prankweb based on machine learning method



**Table 2.** Binding sites detected by Prankweb in CEACAM 1 (PDB code: 5DZL)

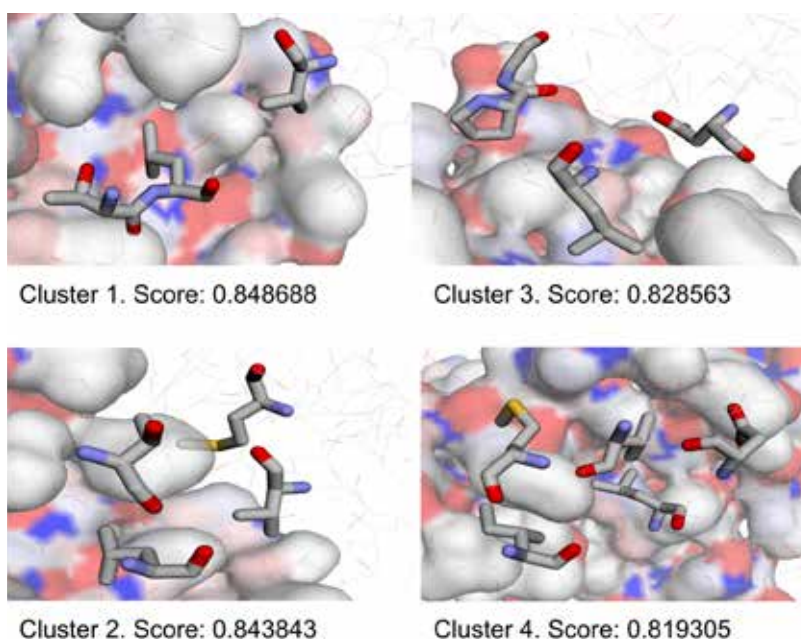
Color	Rank	Score	# of residues
	1	4.04	11
	2	2.27	8
	3	1.09	7

**Virtual Screening:**

By analyzing the interaction between CEACAM1 and HopQ (PDB ID: 7RQR4), PocketQuery identified key amino acid residues involved in their binding. It finds four distinct clusters of interactions, each with a high score (ranging from 0.819305 to 0.848688), indicating strong binding affinities. There are many different amino acids

present in these clusters, with some residues appearing in multiple clusters. Notably, LEU150 and VAL156 are present in three out of four clusters, suggesting they may play a role in the CEACAM1/HopQ interaction. THR appears in both clusters 1 and 2, while MET240 is found in clusters 2 and 4. This overlap indicates that certain amino acids contribute to multiple binding sites.

**Figure 5.** Visual representation of the 4 clusters of the CEACAM1 interaction with HopQ (PDB ID: 7RQR4) using Pocket Query

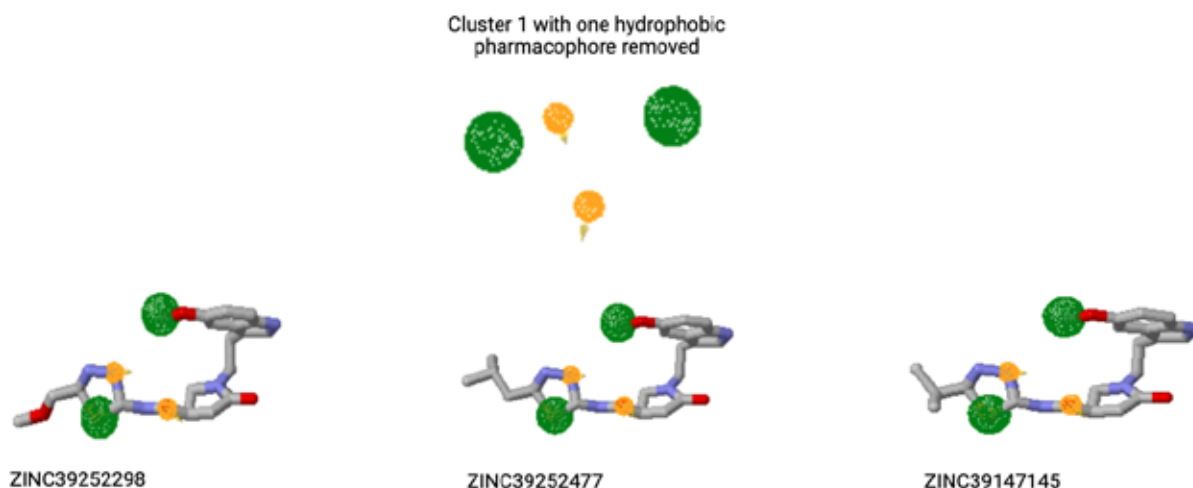


**Table 3.** The amino acids involved in the pharmacophore maps for CEACAM1/HopQ interaction(PDB ID: 7RQR4) found by Pocket Query

Cluster Number	Residues	#
1	THR	149
1	LEU	150
1	VAL	156
2	THR	147
2	LEU	150
2	VAL	156
2	MET	240
3	PRO	110
3	GLY	111
3	ASN	145
3	LEU	150
4	ILE	102
4	LEU	150
4	ASP	153
4	VAL	156
4	MET	240

This part of the experiment identified potential CEACAM1 hits across four distinct clusters using ZincPharmer. Cluster 1 compounds (ZINC39252298, ZINC39252477, ZINC39147145, ZINC39147149, ZINC39252325) all showed consistent RMSD values of 0.151 and masses ranging from 432–448 Da. Cluster 2 compounds (ZINC95379969, ZINC41591046, ZINC81530427, ZINC89851740, ZINC38617077) exhibited the lowest RMSD values (0.002–0.003) and lower masses (343–389 Da), indicating they most closely match the target pharmacophore and may have favorable drug-like proper-

ties. Cluster 3 compounds (ZINC67902861, ZINC71788521, ZINC80694653, ZINC80695211, ZINC08376405) showed intermediate RMSD values (0.047–0.067) and a wide mass range (332–653 Da). Cluster 4 compounds (ZINC08449618, ZINC36047021, ZINC36047023, ZINC08820313, ZINC08449640) had the highest RMSD values (0.152–0.199) and relatively high masses (478–592 Da). The outcome suggests that Cluster 2 compounds, particularly ZINC95379969 and ZINC41591046, are the most promising leads for CEACAM1 inhibition due to their fit to the pharmacophore model.

**Figure 6.** Top compounds as potential CEACAM1 hits with the lowest RMSD from each cluster selected using ZINCPharmer



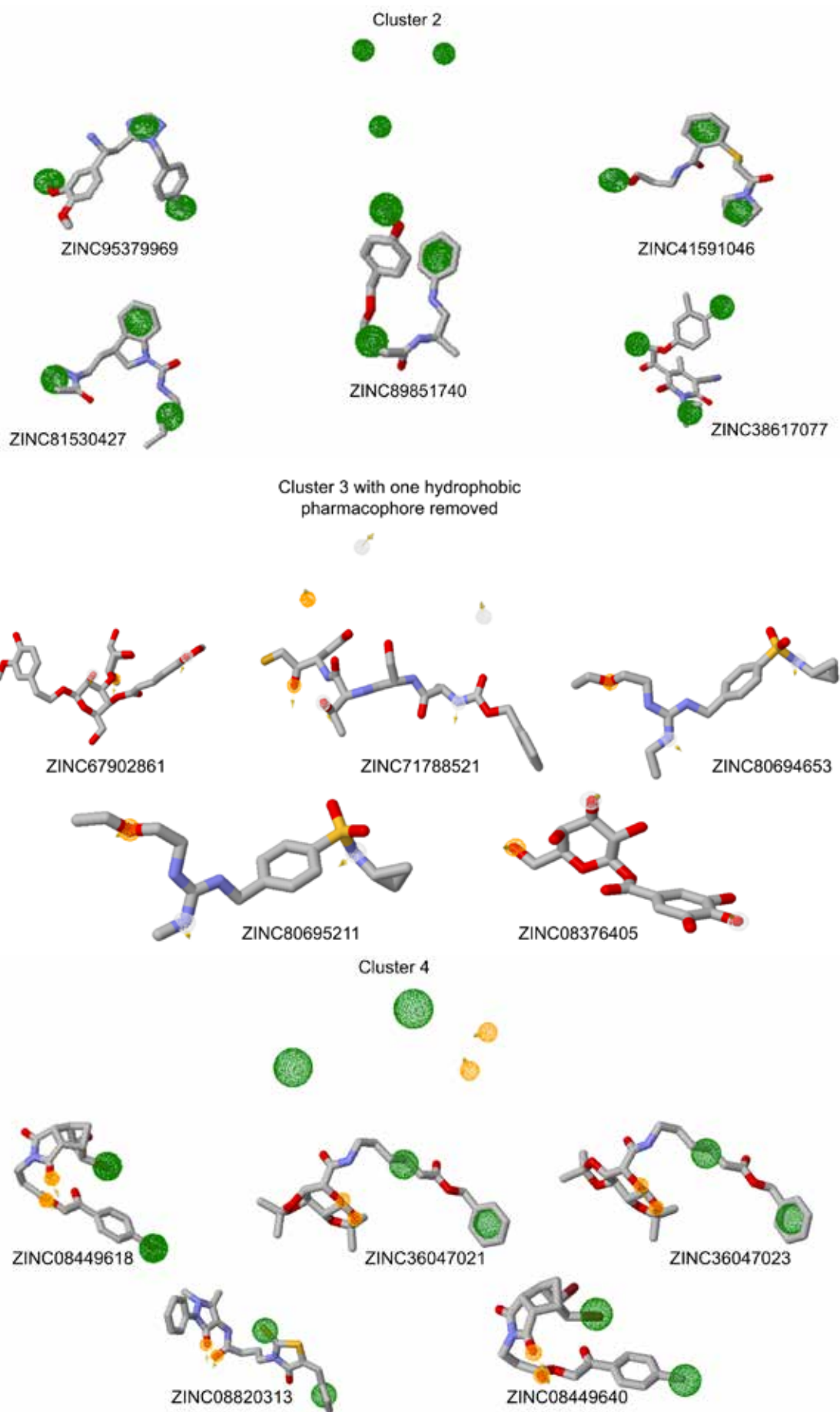


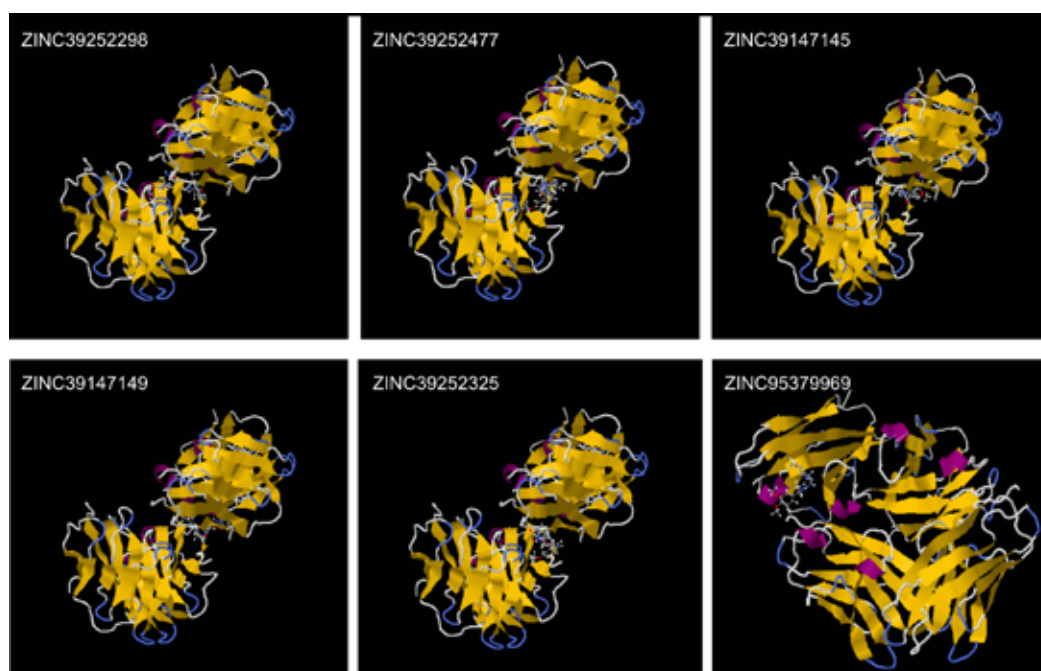
**Table 4.** Top 20 potential CEACAM1 hits with the lowest RMSD from each cluster using ZINCPharmer

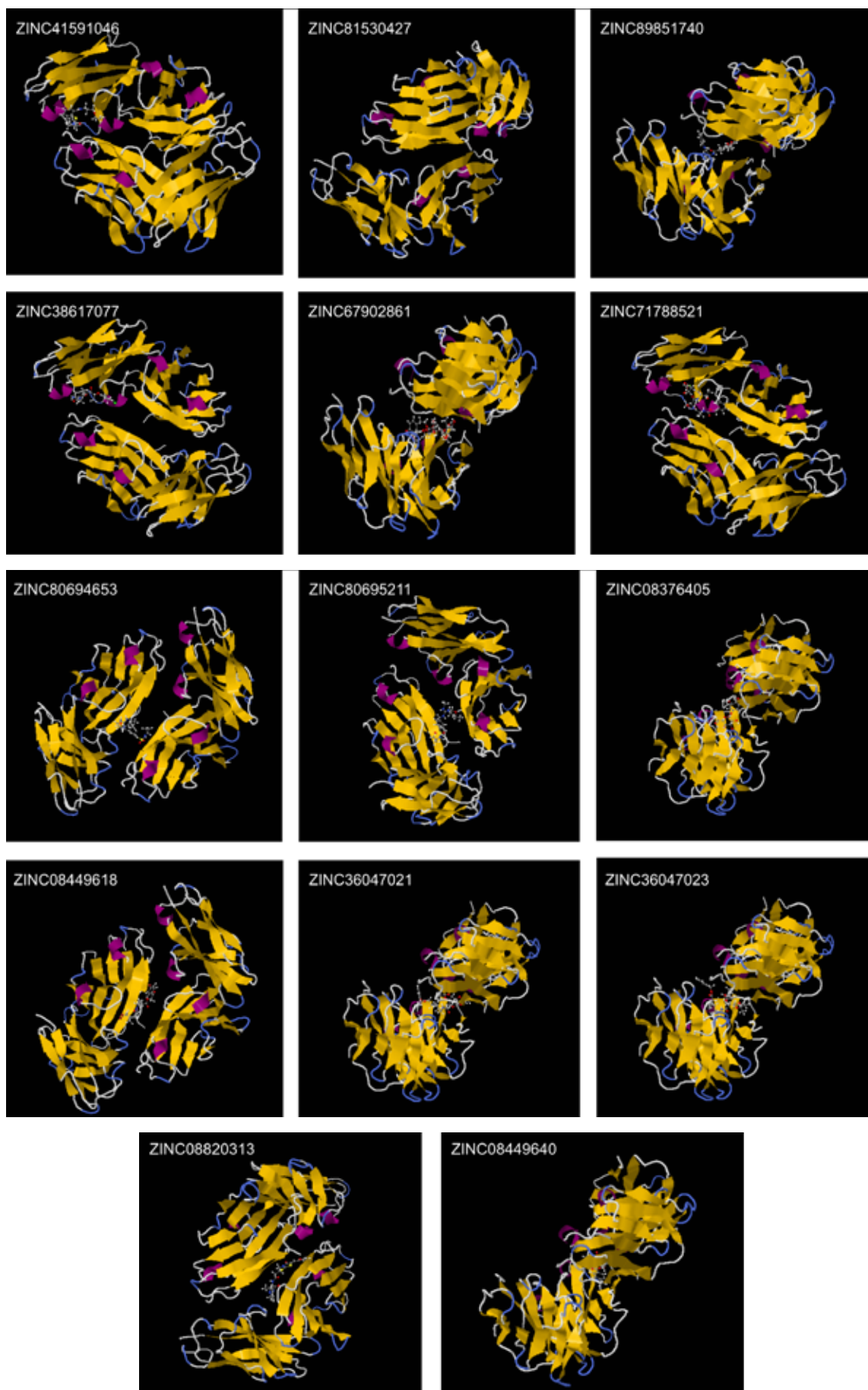
Cluster Number	Name	RMSD	Mass
1	ZINC39252298	0.151	434
1	ZINC39252477	0.151	446
1	ZINC39147145	0.151	432
1	ZINC39147149	0.151	446
1	ZINC39252325	0.151	448
2	ZINC95379969	0.002	353
2	ZINC41591046	0.002	350
2	ZINC81530427	0.003	343
2	ZINC89851740	0.003	356
2	ZINC38617077	0.003	389
3	ZINC67902861	0.047	653
3	ZINC71788521	0.047	542
3	ZINC80694653	0.062	370
3	ZINC80695211	0.062	355
3	ZINC08376405	0.067	332
4	ZINC08449618	0.152	592
4	ZINC36047021	0.179	478
4	ZINC36047023	0.181	478
4	ZINC08820313	0.191	483
4	ZINC08449640	0.199	527

**Molecular Docking:**

This experiment found the estimated binding energies ( $\Delta G$ ) between CEACAM1 and other compounds, aiming to identify

suitable drug candidates. The top 5 compounds with the most favorable (most negative) estimated  $\Delta G$  values are highlighted in yellow:

**Figure 7.** Quantifying the energy between CEACAM1 and compounds, therefore choosing suitable drug candidates



ZINC71788521 (Cluster number 3): -10.90 kcal/mol  
 ZINC67902861 (Cluster number 3): -10.00 kcal/mol  
 ZINC08820313 (Cluster number 4): -9.97 kcal/mol  
 ZINC38617077 (Cluster number 2): -9.89 kcal/mol

ZINC41591046 (Cluster number 2): -9.39 kcal/mol

These compounds show the strongest predicted binding to CEACAM1, with ZINC71788521 exhibiting the most favorable interaction.

**Table 5.** Quantifying the energy between CEACAM1 and compounds, therefore choosing suitable drug candidates (top 5 estimated  $\Delta G$  highlighted in yellow)

ZINC id	Cluster	Estimated $\Delta G$ (kcal/mol)
ZINC39252298	15	-8.47
ZINC39252477	1	-8.55
ZINC39147145	6	-8.77
ZINC39147149	9	-8.26
ZINC39252325	7	-8.75
ZINC95379969	19	-9.0
<b>ZINC41591046</b>	<b>1</b>	<b>-9.39</b>
ZINC81530427	0	-8.03
<b>ZINC89851740</b>	<b>4</b>	<b>-8.50</b>
<b>ZINC38617077</b>	<b>0</b>	<b>-9.89</b>
<b>ZINC67902861</b>	<b>1</b>	<b>-10.00</b>
ZINC71788521	9	-10.90
ZINC80694653	26	-9.19
ZINC80695211	5	-9.24
ZINC08376405	8	-8.04
ZINC08449618	18	-8.50
ZINC36047021	16	-8.51
ZINC36047023	28	-8.49
<b>ZINC08820313</b>	<b>2</b>	<b>-9.97</b>
ZINC08449640	2	-7.94

#### Drug Properties:

This experiment shows the drug properties of the top 5 drug candidates selected for this experiment. The first two candidates (ZINC71788521 and ZINC67902861) violate Lipinski's rule of 5. The violations are due to their high number of H-bond acceptors (11 and 15 respectively) and molecular weights exceeding 500 g/mol. The remaining three candidates (ZINC08820313,

ZINC38617077, and ZINC41591046) comply with Lipinski's rule, having 0 violations, and are classified as drug-like. In conclusion, while the top two candidates show promising target affinity (as implied by their ranking), their drug-like properties are less ideal. The other three candidates offer better drug-like characteristics, making them possibly more suitable for further development.



**Table 6.** *Inspecting the drug properties of the top 5 drug candidates chosen (violations of Lipinski's rule of 5 is highlighted in red)*

ZINC id	Num. H-bond acceptors	Num. H-bond donors	Molecular weight g/mol	iLOGP	Num of violations	Druglike-ness
ZINC71788521	<b>11</b>	<b>6</b>	<b>541.50</b>	0.68	3	No
ZINC67902861	<b>15</b>	<b>7</b>	<b>652.64</b>	3.12	3	No
ZINC08820313	4	1	482.58	3.27	0	Yes
ZINC38617077	5	0	387.84	2.89	0	Yes
ZINC41591046	3	1	350.48	3.44	0	Yes

**Toxicity Prediction:**

In experiment 3.5.1., ZINC08820313 was selected for toxicity assessment using ProTox 3.0 due to its high  $\Delta G$ . The results show a relatively low predicted LD50(3000 mg/kg) and a high toxicity class(5), which are favorable attributes for drug development. In figure 4.5.1, most probabilities for toxic activity are below the average active molecule thresh-

olds, indicating that ZINC08820313 shows little toxic behavior. Although the respiratory toxicity probability is slightly above average, it remains within acceptable limits. Furthermore, as shown in table 4.5.2 and figure 4.5.2, the compound demonstrates a low number of active/toxic sites. This shows the potential of ZINC08820313 as a viable drug candidate with manageable toxicity risks.

**Table 7.** *Summary of toxicity of selected compound(ZINC08820313) using ProTox 3.0*

Predicted LD50(mg/kg)	Predicted toxicity class
3000	5

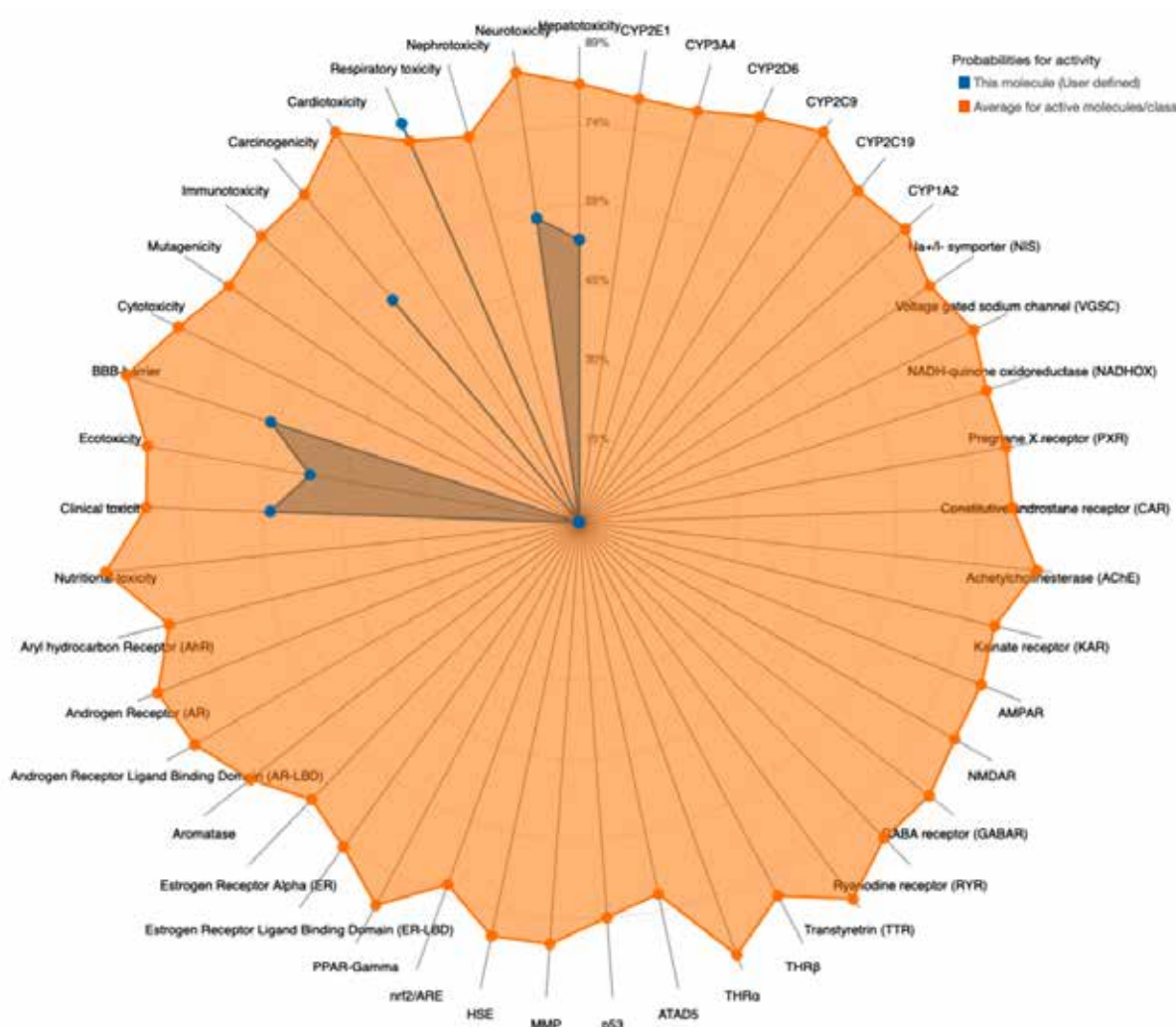
**Table 8.** *Detailing active and inactive parts of ZINC08820313 to measure toxicity (with active parts highlighted in red)*

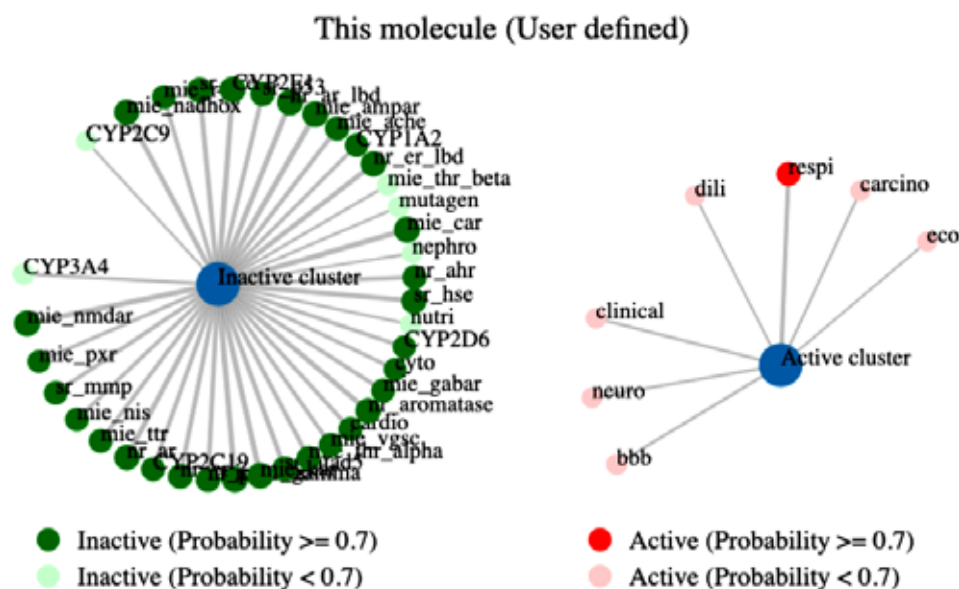
Classification	Target	Shorthand	Prediction
<b>Organ toxicity</b>	<b>Hepatotoxicity</b>	<b>dili</b>	<b>Active</b>
<b>Organ toxicity</b>	<b>Neurotoxicity</b>	<b>neuro</b>	<b>Active</b>
Organ toxicity	Nephrotoxicity	nephro	Inactive
<b>Organ toxicity</b>	<b>Respiratory toxicity</b>	<b>respi</b>	<b>Active</b>
Organ toxicity	Cardiotoxicity	cardio	Inactive
<b>Toxicity end points</b>	<b>Carcinogenicity</b>	<b>carcino</b>	<b>Active</b>
Toxicity end points	Immunotoxicity	immuno	Inactive
Toxicity end points	Mutagenicity	mutagen	Inactive
Toxicity end points	Cytotoxicity	cyto	Inactive
<b>Toxicity end points</b>	<b>BBB-barrier</b>	<b>bbb</b>	<b>Active</b>
<b>Toxicity end points</b>	<b>Ecotoxicity</b>	<b>eco</b>	<b>Active</b>
<b>Toxicity end points</b>	<b>Clinical toxicity</b>	<b>clinical</b>	<b>Active</b>
Toxicity end points	Nutritional toxicity	nutri	Inactive
Tox21-Nuclear receptor signalling pathways	Aryl hydrocarbon Receptor (AhR)	nr_ahr	Inactive
Tox21-Nuclear receptor signalling pathways	Androgen Receptor (AR)	nr_ar	Inactive

<b>Classification</b>	<b>Target</b>	<b>Shorthand</b>	<b>Prediction</b>
Tox21-Nuclear receptor signalling pathways	Androgen Receptor Ligand Binding Domain (AR-LBD)	nr_ar_lbd	Inactive
Tox21-Nuclear receptor signalling pathways	Aromatase	nr_aromatase	Inactive
Tox21-Nuclear receptor signalling pathways	Estrogen Receptor Alpha (ER)	nr_er	Inactive
Tox21-Nuclear receptor signalling pathways	Estrogen Receptor Ligand Binding Domain (ER-LBD)	nr_er_lbd	Inactive
Tox21-Nuclear receptor signalling pathways	Peroxisome Proliferator Activated Receptor Gamma (PPAR-Gamma)	nr_ppar_gamma	Inactive
Tox21-Stress response pathways	Nuclear factor (erythroid-derived 2)-like 2/antioxidant responsive element (nrf2/ARE)	sr_are	Inactive
Tox21-Stress response pathways	Heat shock factor response element (HSE)	sr_hse	Inactive
Tox21-Stress response pathways	Mitochondrial Membrane Potential (MMP)	sr_mmp	Inactive
Tox21-Stress response pathways	Phosphoprotein (Tumor Suppressor) p53	sr_p53	Inactive
Tox21-Stress response pathways	ATPase family AAA domain-containing protein 5 (ATAD5)	sr_atad5	Inactive
Molecular Initiating Events	Thyroid hormone receptor alpha (THR $\alpha$ )	mie_thr_alpha	Inactive
Molecular Initiating Events	Thyroid hormone receptor beta (THR $\beta$ )	mie_thr_beta	Inactive
Molecular Initiating Events	Transthyretin (TTR)	mie_ttr	Inactive
Molecular Initiating Events	Ryanodine receptor (RYR)	mie_ryr	Inactive
Molecular Initiating Events	GABA receptor (GABAR)	mie_gabar	Inactive
Molecular Initiating Events	Glutamate N-methyl-D-aspartate receptor (NMDAR)	mie_nmdar	Inactive
Molecular Initiating Events	alpha-amino-3-hydroxy-5-methyl-4-isoxazole-propionate receptor (AMPA)	mie_ampar	Inactive
Molecular Initiating Events	Kainate receptor (KAR)	mie_kar	Inactive
Molecular Initiating Events	Achetylcholinesterase (AChE)	mie_ache	Inactive
Molecular Initiating Events	Constitutive androstane receptor (CAR)	mie_car	Inactive
Molecular Initiating Events	Pregnane X receptor (PXR)	mie_pxr	Inactive

Classification	Target	Shorthand	Prediction
Molecular Initiating Events	NADH-quinone oxidoreductase (NADHOX)	mie_nadhox	Inactive
Molecular Initiating Events	Voltage gated sodium channel (VGSC)	mie_vgsc	Inactive
Molecular Initiating Events	Na <sup>+</sup> /I <sup>-</sup> symporter (NIS)	mie_nis	Inactive
Metabolism	Cytochrome CYP1A2	CYP1A2	Inactive
Metabolism	Cytochrome CYP2C19	CYP2C19	Inactive
Metabolism	Cytochrome CYP2C9	CYP2C9	Inactive
Metabolism	Cytochrome CYP2D6	CYP2D6	Inactive
Metabolism	Cytochrome CYP3A4	CYP3A4	Inactive
Metabolism	Cytochrome CYP2E1	CYP2E1	Inactive

**Figure 8.** Toxicity radar chart comparing the probabilities for activity in ZINC08820313 and average active molecules



**Figure 9.** Network chart visually illustrating the active and inactive parts of ZINC08820313

### 5. Conclusion:

This study successfully identified several promising drug candidates targeting CEACAM1 through an extensive computational screening process. The primary objectives of this research were to identify compounds with high binding affinity for CEACAM1 and to evaluate their drug-like properties and toxicity profiles. The compounds ZINC71788521 and ZINC67902861, while initially promising due to their strong target affinities, were found to violate Lipinski's rules, thus making them not suitable as drug candidates. In contrast, ZINC08820313, ZINC38617077, and ZINC41591046 demonstrated strong binding potential and adhered to the pharmacokinetic properties outlined by Lipinski. After comparing toxicity and estimated  $\Delta G$  values, ZINC08820313 was selected as the final drug candidate. By targeting an immune checkpoint molecule, the drug candidate offers an approach to overcoming immune evasion by cancer cells, potentially improving patient outcomes in cancer therapy. The drug-like properties of the identified compound suggest its potential for clinical application. With further development and testing, it could be integrated into existing cancer treatment regimens, allowing different combination therapies with immunotherapy targeting CEACAM1.

In the future, focus will be on conducting in vitro experiments to verify the binding affini-

ties of ZINC08820313 with CEACAM1. These experiments will help establish the efficacy of these compounds in a controlled biological environment. If successful in vitro validation, in vivo studies are necessary to evaluate the pharmacokinetics, bioavailability, and therapeutic efficacy of the identified compounds in animal models. Later, if in vivo experiment successes, clinical trials should be conducted, which could lead to the development of more comprehensive and effective cancer treatment protocols. While the study presents promising candidates for cancer immunotherapy, it is important to acknowledge certain limitations. First, this study relies heavily on computational methods for initial screening and evaluation. Although these methods provide valuable insights, experimental validation is essential to confirm the accuracy and applicability of the predictions. Secondly, cancer is a multifaceted disease, and targeting a single molecule may not be sufficient for effective treatment in all cases. A multi-target approach or combination therapies may be necessary to address the diverse mechanisms of cancer progression and immune evasion.

In conclusion, this research has laid a solid foundation for the development of CEACAM1-targeted therapies in cancer immunotherapy. The identification of ZINC08820313 as a promising drug candidate highlights the potential of targeting immune checkpoints to enhance the body's natural defense against



cancer. By continuing to explore innovative therapeutic strategies, the aim is to contribute to the ongoing efforts in developing more

effective and less toxic cancer treatments, ultimately improving the quality of life for cancer patients worldwide.

## References

- Alsaab, H. O., Sau, S., Alzhrani, R., Tatiparti, K., Bhise, K., Kashaw, S. K., & Iyer, A. K. (2017). PD-1 and PD-L1 Checkpoint Signaling Inhibition for Cancer Immunotherapy: Mechanism, Combinations, and Clinical Outcome. *Frontiers in Pharmacology*, – 8(561).
- Benchimol, S., Fuks, A., Jothy, S., Beauchemin, N., Shiota, K., & Stanners, C. P. (1989). Carcinoembryonic antigen, a human tumor marker, functions as an intercellular adhesion molecule. *Cell*, – 57(2), 327–334.
- Brümmer, J., Ebrahimnejad, A., Flayeh, R., Schumacher, U., Löning, T., Bamberger, A. M., & Wagener, C. (2001). cis Interaction of the cell adhesion molecule CEACAM1 with integrin beta(3). *The American journal of pathology*, – 159(2), 537–546.
- Buchbinder, E. I., & Desai, A. (2016). CTLA-4 and PD-1 Pathways: Similarities, Differences, and Implications of Their Inhibition. *American journal of clinical oncology*, – 39(1), 98–106.
- Cancer Research UK. (2023, October 28). Types of Cancer. Cancer Research UK. Assessed on June 24th 2024. Retrieved from URL: <https://www.cancerresearchuk.org/about-cancer/what-is-cancer/how-cancer-starts/types-of-cancer>
- Chaitanya Thandra, K., Barsouk, A., Saginala, K., Sukumar Aluru, J., & Barsouk, A. (2021). Epidemiology of lung cancer. *Współczesna Onkologia*, – 25(1), 45–52.
- Dankner, M., Gray-Owen, S. D., Huang, Y. H., Blumberg, R. S., & Beauchemin, N. (2017). CEACAM1 as a multi-purpose target for cancer immunotherapy. *Oncoimmunology*, – 6(7), e1328336.
- Darvin, P., Toor, S. M., Sasidharan Nair, V., & Elkord, E. (2018). Immune checkpoint inhibitors: recent progress and potential biomarkers. *Experimental & molecular medicine*, – 50(12), 1–11.
- Helfrich, I., & Singer, B. B. (2019). Size Matters: The Functional Role of the CEACAM1 Isoform Signature and Its Impact for NK Cell-Mediated Killing in Melanoma. *Cancers*, – 11(3), 356.
- Hodi, F. S., O'Day, S. J., McDermott, D. F., Weber, R. W., Sosman, J. A., Haanen, J. B., Gonzalez, R., Robert, C., Schadendorf, D., Hassel, J. C., Akerley, W., van den Eertwegh, A. J., Lutzky, J., Lorigan, P., Vaubel, J. M., Linette, G. P., Hogg, D., Ottensmeier, C. H., Lebbé, C., Peschel, C., ... Urba, W. J. (2010). Improved survival with ipilimumab in patients with metastatic melanoma. *The New England journal of medicine*, – 363(8), 711–723.
- Horst, A. K., Bickert, T., Brewig, N., Ludewig, P., van Rooijen, N., Schumacher, U., Beauchemin, N., Ito, W. D., Fleischer, B., Wagener, C., & Ritter, U. (2009). CEACAM1+ myeloid cells control angiogenesis in inflammation. *Blood*, – 113(26), 6726–6736.
- Kim, W. M., Huang, Y.-H., Gandhi, A., & Blumberg, R. S. (2019). CEACAM1 structure and function in immunity and its therapeutic implications. *Seminars in Immunology*, – 42, 101296.
- Klaile, E., Vorontsova, O., Sigmundsson, K., Müller, M. M., Singer, B. B., Ofverstedt, L. G., Svensson, S., Skoglund, U., & Obrink, B. (2009). The CEACAM1 N-terminal Ig domain mediates cis- and trans-binding and is essential for allosteric rearrangements of CEACAM1 microclusters. *The Journal of cell biology*, – 187(4), 553–567.
- Markel, G., Seidman, R., Cohen, Y., Besser, M. J., Sinai, T. C., Treves, A. J., Orenstein, A., Berger, R., & Schachter, J. (2009). Dynamic expression of protective CEACAM1 on melanoma cells during specific immune attack. *Immunology*, – 126(2), 186–200.
- Nagaishi, T., Chen, Z., Chen, L., Iijima, H., Nakajima, A., & Blumberg, R. S. (2008). CEACAM1 and the regulation of mucosal inflammation. *Mucosal Immunology*, – 1(1), S39–S42.
- National Cancer Institute. (2018). Cancer of the Lung and Bronchus – Cancer Stat Facts. National Cancer Institute. Accessed on June 18<sup>th</sup> 2024. Retrieved from URL: – <https://seer.cancer.gov/statfacts/html/lungb.html>
- Park, D. J., Sung, P. S., Kim, J. H., Lee, G. W., Jang, J. W., Jung, E. S., Bae, S. H., Choi, J. Y., & Yoon, S. K. (2020). EpCAM-high liver cancer stem cells resist natural killer cell-mediated

- ed cytotoxicity by upregulating CEACAM1. *Journal for immunotherapy of cancer*, – 8(1), e000301.
- Pauken, K. E., & Wherry, E. J. (2015). Overcoming T cell exhaustion in infection and cancer. *Trends in immunology*, – 36(4), 265–276.
- Tsang, K. Y., Fantini, M., Mavroukakis, S. A., Zaki, A., Annunziata, C. M., & Arlen, P. M. (2022). Development and Characterization of an Anti-Cancer Monoclonal Antibody for Treatment of Human Carcinomas. *Cancers*, – 14(13), 3037.
- Turcu, G., Nedelcu, R. I., Ion, D. A., Brînzea, A., Cioplea, M. D., Jilaveanu, L. B., & Zurac, S. A. (2016). CEACAM1: Expression and Role in Melanocyte Transformation. *Disease markers*, 2016, – 9406319.
- Zappasodi, R., Merghoub, T., & Wolchok, J. D. (2018). Emerging Concepts for Immune Checkpoint Blockade-Based Combination Therapies. *Cancer Cell*, 34(4), 690.
- Zhang, Y., & Zhang, Z. (2020). The history and advances in cancer immunotherapy: understanding the characteristics of tumor-infiltrating immune cells and their therapeutic implications. *Cellular & Molecular Immunology*, – 17(8), 1–15.

submitted 12.09.2024;  
accepted for publication 29.09.2024;  
published 29.10.2024  
© Guanrong (Rain) Cheng  
Contact: raincheng08@gmail.com